



# Experimental compaction of anisotropic granular media

Philippe Ribière, Patrick Richard, Daniel Bideau, Renaud Delannay

## ► To cite this version:

Philippe Ribière, Patrick Richard, Daniel Bideau, Renaud Delannay. Experimental compaction of anisotropic granular media. 2005. hal-00004376

**HAL Id: hal-00004376**

**<https://hal.science/hal-00004376>**

Preprint submitted on 7 Mar 2005

**HAL** is a multi-disciplinary open access archive for the deposit and dissemination of scientific research documents, whether they are published or not. The documents may come from teaching and research institutions in France or abroad, or from public or private research centers.

L'archive ouverte pluridisciplinaire **HAL**, est destinée au dépôt et à la diffusion de documents scientifiques de niveau recherche, publiés ou non, émanant des établissements d'enseignement et de recherche français ou étrangers, des laboratoires publics ou privés.

# Experimental compaction of anisotropic granular media

Philippe Ribière, Patrick Richard, Daniel Bideau and Renaud Delannay

Groupe Matière Condensée et Matériaux, UMR CNRS 6626, Université de Rennes 1, Campus de Beaulieu, F-35042 Rennes cedex, France

**Abstract.** We report on experiments to measure the temporal and spatial evolution of packing arrangements of anisotropic and weakly confined granular material, using high-resolution  $\gamma$ -ray adsorption. In these experiments, the particle configurations start from an initially disordered, low-packing-fraction state and under vertical solicitations evolve to a dense state. We find that the packing fraction evolution is slowed by the grain anisotropy but, as for spherically shaped grains, can be well fitted by a stretched exponential. For a given type of grains, the characteristic times of relaxation and of convection are found to be of the same order of magnitude. On the contrary compaction mechanisms in the media strongly depend on the grain anisotropy.

**PACS.** 45.70.-n Granular systems. – 45.70.Cc Static sandpiles; granular compaction – 81.05 Porous materials; granular materials

## 1 Introduction

Granular media are not thermal systems: the thermal energy  $k_B T$  is not involved in the evolution because it is negligible compared to the variation of the gravitational energy during the motion of a grain. Nevertheless they share with glasses a great number of properties - such as off equilibrium dynamics, aging and hysteresis. . . It has even been suggested that the relaxation of a granular medium under weak mechanical perturbations, such as shaking, has a formal analogy with the slow dynamics of out-of-equilibrium thermal systems [1,2]. This analogy is based on the assumption that the most important parameter in the system is the geometry and not the interaction between particles or the driving energy. Consequently, although mechanical agitation is neither stochastic nor isotropic, relaxation of granular media is often presented as an ideal system to study out-of-equilibrium dynamics [3].

The first experiments of slow relaxation in granular media submitted to external mechanical excitations have been carried out in Chicago [4,5]. By implementing, at regular intervals, identical vertical taps of controlled intensity, they show that the packing fraction of the media increases slowly with the number of taps. This has been done for both spherical [4] and anisotropic grains [5]. For isotropic grains, the evolution of the strongly confined media is correctly described by the inverse of the logarithm of the number of taps described in equation (1):

$$\Phi = \Phi_\infty - (\Phi_\infty - \Phi_0) \frac{1}{1 + B \ln(1 + t/\tau)}. \quad (1)$$

The four parameters adjusted during the fit are  $\Phi_0$  the initial packing fraction,  $\Phi_\infty$  the final packing fraction (for

$t \rightarrow \infty$ ),  $\tau$ , a characteristic time of the evolution and  $B$  a parameter without any physical interpretation.

Other experiments have been carried out in quite different systems: compaction under shearing [6,7] or under tapping but with a larger vessel [8,9,10,11] - and thus a weaker confinement - than the one used in [4]. In [8] the best fit found is not the one used by the Chicago group but the so called KWW's fit (Kohlrausch, Williams, Watts) [12,13]. This law is a stretched exponential (Eq. 2):

$$\Phi = \Phi_\infty - (\Phi_\infty - \Phi_0) \exp(-(t/\tau)^\beta), \quad (2)$$

where  $\tau$  is a characteristic time and  $\beta$  measures the slowing down compared to the simple exponential law. Here  $\Phi_0$  and  $\Phi_\infty$  are not fit parameters but experimental data:  $\Phi_0$  is the first point of the curve (the initial packing fraction) and  $\Phi_\infty$  the mean value of the packing fraction at the stationary state. The tapping intensity is found to rule the characteristic time of relaxation according to an Arrhenius behavior relation. All these characteristics are similar to those obtained in strong glassy systems and thus these results confirm the analogy between glasses and granular media explained in the introduction.

The aim of this article is to check the validity of the results obtained in [8,9] with non-spherical shaped grains. Indeed, to reduce the number of parameters, most previous studies deal with spherical grains [4,6,7,8,10,9,11]. Nevertheless actual granular material are far from being perfectly isotropic. Grain anisotropy modify geometrical frustration and may change packing behavior and convection during compaction.

This paper is organized as follows. In the next section, the experimental setup is described. Results on the relaxation and on the dynamics of compaction are shown

in section 3. The last section contains a summary of the findings and conclusions.

## 2 Experimental setup

The experimental setup consists of a glass cylinder of diameter  $D \approx 10$  cm filled with about 600 g of grains (corresponding to a height of roughly 10 cm). The method used to build our initial packing, already used for spheres [8,9], is reproducible (we obtain the same initial packing fraction and the same packing fraction evolution for a given tapping amplitude). It consists of using two grids. The first one is placed at the bottom and inside the cylinder. The grains are then poured through the second one which is placed at the top the container. Once the filling procedure is finished, the first grid is pulled through the medium which is then diluted. This allows to obtain a low initial packing fraction.

The container is placed on the plate connected to an electromagnetic exciter (LDS V406) which induces a vertical displacement of the plate. The container is in this way shaken at regular intervals ( $\Delta t = 1$  s) by vertical taps. Each tap is created by selecting an entire period of sine wave at a constant frequency  $f = 30$  Hz. The resulting motion of the whole system, monitored by an accelerometer at the bottom of the container, is however more complicated than a simple sine wave. At first, the system undergoes a positive acceleration followed by a negative peak with a minimum equal to  $-\gamma_{max}$  as showed in Figure 1. Moreover, it can be seen on this figure that the acceleration created by the fall of the media on the bottom of the cylinder,  $-\gamma_{fall}$ , may be different from  $-\gamma_{max}$ . Indeed we only used taps for which the media took off from the bottom of the glass cylinder. It means the tap intensity is always chosen upon the lift-off threshold. After the applied voltage stops, the system relaxes to its normal repose position. Sequences of  $10^4$  to  $10^6$  taps are carried out with

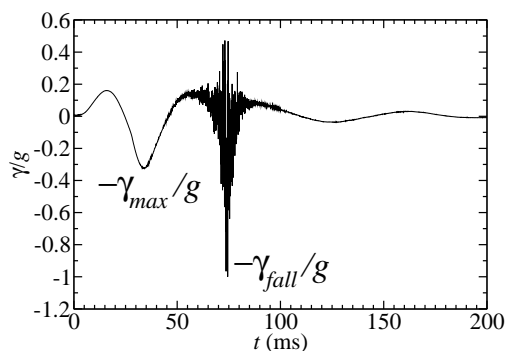


**Fig. 1.** Example of dynamical signal monitored by the accelerometer for  $\Gamma \approx 3.5$ . The acceleration created by the fall of the media on the bottom  $-\gamma_{fall}$  is different from the minimal acceleration applied to the system  $\gamma_{max}$ .

an intensity  $\Gamma$  defined as follows:  $\Gamma = \gamma_{max}/g$  where  $g$  is the gravitational acceleration. Here we call "time" the

number of taps and the "dynamics" is the succession of static equilibrium induced by the taps.

The average volume fraction in the bulk  $\Phi$  is measured using the transmission ratio of  $\gamma$ -ray beam through the media. This setup allows to determine the vertical density profile too. The link between  $\Phi$  and the ratio  $N/N_0$ , where  $N$  and  $N_0$  are the activities counted respectively by the detector with and without media, is:  $\Phi \approx \frac{1}{\mu} \ln(N/N_0)$ . In this equation,  $\mu$  is the absorption coefficient of the beads determined experimentally [8,9]. The collimated  $\gamma$ -beam is nearly cylindrical with a diameter of 10 mm and intercepts perpendicularly the vertical axis of the cylindrical container. An acquisition-time of 60 s was found to be a good compromise between the intrinsic uncertainty of a radioactive beam and the total duration of an experiment. We then achieve a precision  $\Delta\Phi = \pm 0.003$ . With the aim of limiting the duration of the experiments (from 20 hours to more than a month according to the total number of taps) and of avoiding redundant information due to the very slow evolution of the system, the measurements are spaced out in time, on a logarithmic scale, with 2 measures of packing fraction profile and 50 measures of mean packing fraction of the sample  $\langle\Phi\rangle$  per decade (except 10 for the first decade).

The anisotropic grains used are rices of different shapes (see Fig. 2): long grains (basmati rice) and short grains (round rice). Results obtained with spheres in previous works [8,9] are also reported. In order to quantify the grain



**Fig. 2.** Picture of the grains used: basmati rice (left), round rice (center) and glass beads (right)

anisotropy each grain is assimilated to an ellipsoid and the mean ratio between the two axis is measured. We obtain 2.5 for the basmati rice and 1.5 for the round rice. It is worth noting that the size distribution is larger for the round rice (size dispersion around 20%) than for the basmati rice (less than 10%).

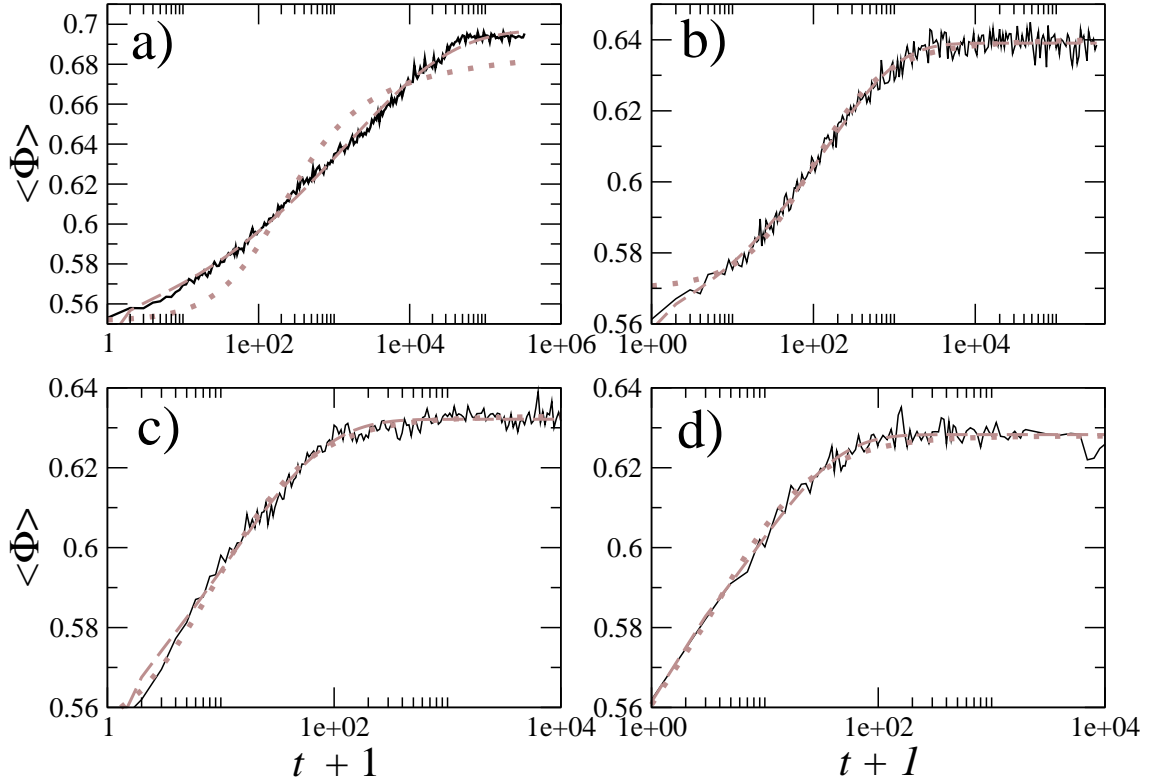


**Fig. 3.** Evolution of the packing fraction of a) basmati rice with  $\Gamma = 2.4$ , b) round rice with  $\Gamma = 2.4$ , c) basmati rice with  $\Gamma = 6$  and d) round rice with  $\Gamma = 6$ . Chicago group's fit (dotted line) and KWW's fit (dashed line) are reported for each curve. For all the fits we used the Levenberg-Marquardt algorithm and the parameters  $\Phi_0$  and  $\Phi_\infty$  are set to the experimental values.

### 3 Dynamics of compaction

#### 3.1 influence of the shape on the initial and final packing fraction

For disordered packings of spheres, computer simulations as well as experiments have shown that the maximal packing fraction is set by the so-called random close packing (RCP) ( $\Phi \approx 0.64$ ). Moreover the minimal packing fraction for a mechanically stable sphere packing (the random loose packing) is often set to  $\Phi \approx 0.55$ . Such estimations for disordered packings do not exist for anisotropic-grain packings. As mentioned above, the method used to build our initial packing is reproducible. It gives  $\Phi \approx 0.56$  for round rice and  $\Phi \approx 0.55$  for basmati rice, which means that, in our experiments, the more anisotropic the grains are, the less important the initial packing fraction is. This can be explained by the fact that arches - and thus large pores - form more easily with anisotropic grains. Figure 3 reports the evolution of the packing fraction with the number of taps for the two kinds of rice and for  $\Gamma = 6$  and 2.4. The first observations is that, whereas final packing fractions for round rice are comparable to what is obtained for compaction of sphere packings, they can be much higher for the basmati rice. Nevertheless we do not observe, contrary to Villarruel et al [5], an ordered phase in which the grains align vertically. This order seems to be due to the strong lateral confinement. Indeed in [5] the length of the

rods used is the same as the diameter of the cylinder so the steric constraints are huge. In our experiments the smaller ratio between the diameter of the cylinder and the length of the grain is about 25. Nevertheless, as explained below, we can observe for given values of  $\Gamma$ , an order which is different from that observed in [5].

#### 3.2 Dynamics of compaction for basmati rice

Depending on the value of  $\Gamma$ , two types of phenomena can be observed in basmati rice: for high values of tapping intensity  $\Gamma$ , convection is observed in the whole media whereas for low values of  $\Gamma$  convection is localized in a part of the packing and is not steady. As it will be shown, compaction mechanisms strongly depend on the convection and thus on  $\Gamma$ . It should be pointed out that we only consider values of  $\Gamma$  larger than the lift-off threshold [10]. For high tapping intensity (typically  $\Gamma > 3$ ) convection takes place within the whole medium. After about ten taps, two convection rolls appear but this situation becomes unstable. One of the rolls progressively disappears and after this transient the whole medium is fulfilled by only one roll and the free surface of the medium is tilted from the horizontal (for example about  $20^\circ$  for  $\Gamma = 6$ ). This can be observed at the vessel wall as showed in Figure 4. With regular acquisition of images after each mechanical perturbation, a characteristic time for the evolu-

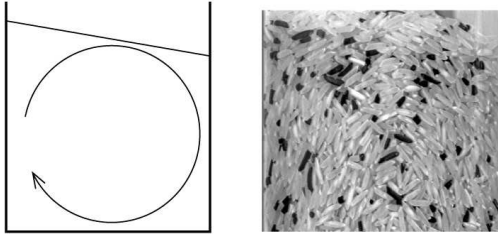


**Fig. 4.** sketch of the convection obtained for basmati rice and for  $\Gamma = 6$  (left) and snapshot of the media during relaxation (right) where convection roll can be clearly seen on the side walls

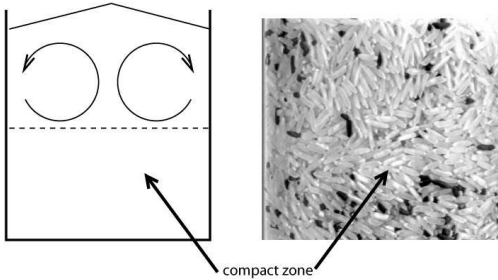


**Fig. 5.** sketch of the convection obtained for basmati rice and for  $\Gamma = 2.4$  (left) and snapshot of the media during relaxation (right) where the compact and ordered part can be clearly seen on the side walls

tion of convection rolls,  $\tau_{conv}$ , can be extracted. Indeed, we can track grain movements at the vessel sides and measure how long it takes a grain to revolve around the center of the convection roll. For basmati rice submitted to taps of intensity  $\Gamma = 6$  we find  $\tau_{conv} \approx 50$ . The evolution of packing fraction during this experiment, is reported in Figure 3c. Chicago group's fit and KWW's fit (using the Levenberg-Marquardt algorithm) both correctly describe the experimental evolution and they give extremely similar correlation coefficients ( $\approx 0.991$ ). However, the evolution of the former fit near the stationary state is slower than the experimental result. The fit provides the following values:  $\tau = 1150$  and  $B = 165$  for Chicago group's law and  $\tau = 30$  and  $\beta = 0.58$  for the KWW's law. The value of  $\tau_{KWW}$  is of the same order of magnitude than  $\tau_{conv}$  and this remains valid for all our experiments done for  $\Gamma > 3$ . Note that for the fits the parameters  $\Phi_\infty$  and  $\Phi_0$  are set to the experimental values.

The behavior of our system is totally different for taps of low intensity ( $\Gamma < 3$ ). Two convection rolls roughly equally-sized and localized near the free surface appear. The other part of this packing (below the rolls) is not submitted to convection. As for the high tapping intensity case, this situation is unstable. Contrary to the previous case the two rolls do not merge: their size continuously decreases until they disappear. For basmati rice and for a solicitation of intensity  $\Gamma = 2.4$ , the convection is stopped in most of the packing after  $\tau \simeq 1500$ . Convection rolls do not exist anymore, except near the air-media interface (see Fig. 5). Another interesting point is that an ordering

process is observed at the bottom of the vessel: the convection rolls compact the lowest part of the packing and align the rice grains horizontally. This explains why the packing fractions obtained can be so high. This order creation is different from that observed by Villarruel et al [5] where the grains are preferentially oriented vertically. Thus the order observed in [5] is created by the side walls whereas the order observed in the present work is created by convection. Note that the aspect ratio of the grains is probably also an important parameter. The evolution of packing fraction during this experiment is showed Figure 3a. On this figure, it can be seen that the fit from Chicago group's law (logarithmic law) does not describe the experimental evolution very well. Indeed, Chicago group's law increases too fast before the steady state and reaches it too late. The parameters of Chicago group's law are  $\tau = 375$  and  $B = 2$  (with a correlation coefficient of 0.972). We recall that for the fit we set the values of  $\Phi_\infty$  equal to the experimental final packing fraction. A better correlation coefficient can be obtained (0.996) if  $\Phi_\infty$  is a free parameter but its value (0.86) is then unrealistic and well above the value of the plateau observed in Figure 3a. So for this law, the parameter  $\tau$  for  $\Gamma = 2.4$  is smaller than  $\tau$  for  $\Gamma = 6$  whereas the evolution slows down with the decrease of  $\Gamma$ . This characteristic time which comes from Chicago group's fit does not show a physical behavior and does not describe our results. On the contrary KWW's law correctly fits the experimental evolution with the following parameters:  $\tau = 1380$  and  $\beta = 0.31$  (with a correlation coefficient of 0.998). Like for the high-intensity solicitations,  $\tau_{KWW}$  the time extracted from KWW's fit and the characteristic time of the convection rolls are similar. So in all our experiment,  $\tau_{KWW}$  can be correlated with a real time of evolution.

It should be pointed out that such kind of correlation is not possible in the experiments of Chicago because the use of a very narrow vessel prevents convection. Therefore the convection mechanisms are not the same in the two setup.

### 3.3 dynamics of compaction for round rice

For round rice, we did not observe the same change of behavior for  $\Gamma \approx 3$ . The convection always took place in the media, as for spherical beads [8,10]. And, as for spherical beads, KWW's fit describes better the experimental evolution of the packing fraction than Chicago group's law (see Figures 3b and 3c). However we could see a strong decrease of the convection speed for intensity taps under  $\Gamma \approx 3$ . More results about convection can be found in [14].

### 3.4 Dependence of the relaxation on $\Gamma$

For our experimental setup, KWW's law is always the best fit. For all the grains used the parameter  $\tau$  follows an Arrhenius behavior (see Fig. 6a)

$$\tau(\Gamma) = \tau_0 \exp\left(\frac{\Gamma_0}{\Gamma}\right). \quad (3)$$

The values of the parameters are  $\tau_0 \approx 1.06$  and  $\Gamma_0 \approx 7$  for glass beads, 1.14 and 12 for short rice and 1.56 and 16 for long rice. Even if the interpretation of  $\tau_0$  is not easy, the value of  $\Gamma_0$  is linked to the height of energy step in the phases space. Indeed, more anisotropic are the beads, larger is the distribution of energy in phases space and so greater must be the typical intensity of a tap to explore this space.

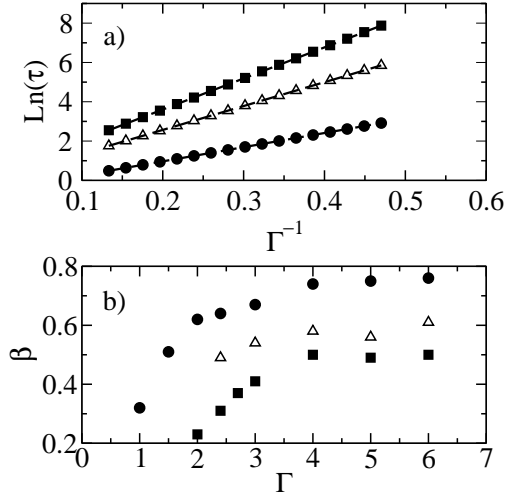


**Fig. 6.** (a) Characteristic time of the stretched exponential as a function of the inverse of the tapping intensity  $\Gamma$  for glass beads (filled circles), round rice (open triangles) and basmati rice (filled squares). (b)  $\beta$  exponent of the stretched exponential fits as function of the tapping intensity  $\Gamma$  for glass beads (filled circles), round rice (triangles) and basmati rice (filled squares). Glass bead data are taken from [8] and [9].

The evolution of  $\beta$  is reported in Figure 6b. It is qualitatively the same for the different kinds of grains. For a given value of tapping intensity  $\Gamma$ , the difference to a perfect exponential ( $\beta = 1$ ) is more important for anisotropic grains. The stretching of the exponential, and thus the coefficient is  $\beta$ , is due to a wide characteristic time dispersion. Since the range of metastable states is wider for anisotropic particles the characteristic times are more dispersed and thus the coefficient  $\beta$  lower.

The last quantity reported is the final packing fraction (Fig. 7). Although the general shape of the curves is similar, the quantitative measures depend on grain shape. Moreover the change of behavior observed for glass beads [8,10] around  $\Gamma \approx 2$  can also be seen for basmati and round rice. This change is very important for basmati rice at  $\Gamma \approx 3$ . The study of a perfect non-inelastic solid on a plate with a sinus motion shows that the flying time does not depend of the solid mass [15]. This explain that the behavior of the glass media and the rice is qualitatively the same with  $\Gamma$ . Nevertheless, a small difference of the threshold between the two regimes is observed but it is due to the change in friction coefficient between the grains and the vessel.

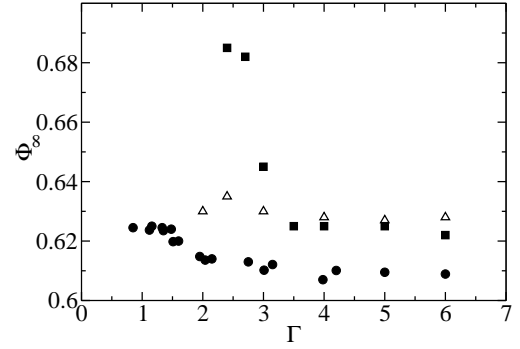


**Fig. 7.** Final packing fraction as a function of the tapping intensity  $\Gamma$  for glass beads (filled circles), round rice (open triangles) and basmati rice (filled squares). Glass bead data are taken from [8] and [9].

## 4 Conclusion

We have studied the effect of grain anisotropy on granular compaction under vertical tapping, and weak lateral confinement. Using a  $\gamma$ -ray adsorption apparatus, we have reported the evolution of the packing fraction as a function of the number of taps. We observe that the main features of granular compaction do not qualitatively depend on grain shape. In particular, the packing fraction evolution can be well fitted by a stretched exponential in all the cases. The fit parameters as well as the final packing fraction have the same qualitative behavior and the fit parameter  $\tau$  is found to be correlated to the experimental characteristic time of the convection. Nevertheless we observed that the convection in the granular media, and thus the compaction mechanisms, strongly depend on grain anisotropy.

## References

1. S.F. Edwards and R.B.S. Oakeshott, *Physica A*, **157**, 1080 (1989); A. Mehta and S.F. Edwards, *Physica A* **157**, 1091 (1989).
2. M. Nicodemi, A. Coniglio and H.J. Herrmann, *Phys. Rev. E*, **55**, 3962 (1997); J. Kurchan, *J. Phys: Cond. Matt.*, **12**, 6611 (2000); A.J. Liu and S.R. Nagel, *Nature*, **396**, 21 (1998).
3. C. Josserand, A.V. Tkachenko, D.M. Mueth and H.M. Jaeger, *Phys. Rev. Letters*, **85**, 3632 (2000).
4. J.B. Knight, C.G. Fandrich, C.N. Lau, H.M. Jaeger and S.R. Nagel, *Phys. Rev. E*, **51**, 3957 (1995); E.R. Nowak, J.B. Knight, E. Ben-Naim, H.M. Jaeger and S.R. Nagel, *Phys. Rev. E* **57**, 1971 (1998).
5. F. X. Villarruel and B. E. Lauderdale and D. M. Mueth and H. M. Jaeger *Phys. Rev. E*. **61**, 6914 (2000).
6. M. Nicolas, P. Duru and O. Pouliquen, *Eur. Phys. J. E* **3**, 309 (2000).
7. O. Pouliquen, M. Belzons and M. Nicolas, *Phys. Rev. Lett.*, **91**, 014301 (2003).
8. P. Philippe and D. Bideau, *Europhys. Letters*, **60**, 677 (2002).

9. P. Philippe Etude théorique et expérimentale de la densification des milieux granulaires. PhD thesis, Université de Rennes 1 (2003).
10. P. Philippe and D. Bideau, Phys. Rev. Lett. **91**, 104302 (2003).
11. P. Richard, P. Philippe, F. Barbe, S. Bourlès, X. Thibault and D. Bideau, Phys. Rev. E, **68**, 020301(R) (2003).
12. R. Kohlrausch, Pogg. Ann. Phys.Chem. **91**, 179 (1854)
13. G. Williams and D.C. Watts, Trans. Faraday Soc. 66, 80 (1970).
14. P. Ribiere, P. Richard, R. Delannay and D. Bideau, Physical Review E, 71, 011304 (2005).
15. A. Mehta and J.M. Luck, Physical Review Letters, **65**, 393-396 (1990).